ATR-IR Fingerprint of Carnauba Wax, obtained by means of a deconvolution based on q-BWF functions and Fityk software

ATR-IR Fingerprint of Carnauba Wax, obtained by means of a deconvolution based on q-BWF functions and Fityk software

Amelia Carolina Sparavigna

Department of Applied Science and Technology, Polytechnic University of Turin, Turin, Italy

Abstract: The fingerprint of an ATR-IR spectrum of Carnauba Wax is proposed. The ATR-IR fingerprint is obtained with a q-BWF functions deconvolution, with these functions implemented in Fityk software. ATR data are Michael Toffolo courtesy.

DOI: 10.5281/zenodo.15183000. Torino, 9 April 2025, amelia.sparavigna@polito.it

Carnauba Wax and its relevance

Carnauba wax is a natural wax derived from the carnauba palm, used in industries for its unique properties. It is used as a hardener, protective coating, and glazing agent in products like car waxes, polishes, cosmetics, food coatings, and pharmaceuticals (de Freitas et al., 2019, Devi et al., 2022, Tinto et al., 2017). That is, this wax is a popular ingredient in car waxes, providing a high-gloss finish and protecting paint from environmental elements like UV rays, rain, and dirt. Carnauba wax is used in lipsticks, lip balms, foundations, and other beauty products for its moisturizing and emollient properties, as well as a thickener. For food industry, it is used as a glazing agent and coating of candies, fruits, and other confectionery products, providing a shiny appearance and extending shelf life (Pashova, 2023). It acts as a tablet-coating agent, making pills easier to swallow, and is also used as a binding agent. Other applications include this wax as a component of furniture, leather, and shoe polishes. It is even relevant as a paper coating (dos Santos et al., 2023, Mendonça et al., 2024). It is used as a hardener for printing inks, painting and a thickener for solvents and oils (Calovi and Rossi, 2023).

IR and Raman spectra

In Bergamonti et al., 2022, we can find interesting research about the identification of waxes in wall paintings from three domus of Herculaneum. “Painting techniques and organic materials of the houses of the Vesuvian area represent fundamental documents for the knowledge of the development of Roman mural painting” (Bergamonti et al., 2022).

As told by Bergamonti and coworkers, “natural waxes are highly heterogeneous materials containing esters of fatty acids with long-chain alcohols, free fatty acids and/or long-chain hydrocarbons. Waxes can be of animal (beeswax, lanolin, spermaceti wax, Chinese wax), vegetable (carnauba, candelilla, esparto wax, Japan wax) and fossil origin (paraffin wax, montan wax, ceresine). Waxes are solid at room temperature, highly hydrophobic, have a plastic character, become soft and workable when warm, have a melting point in the 60–80°C range and are stable to chemical and enzymatic agents” (Bergamonti et al. mentioning Jiménez et al., 2006, Tulloch, 1980, Mills & White, 2012). “The main vegetable waxes carnauba and candelilla are obtained from plants growing in the American continent. Carnauba wax is extracted from the leaves of Copernicia prunifera, a Brazilian palm tree and is the hardest of the vegetable waxes. In restoration practice, carnauba is added to make beeswax harder and increase its melting point” (Bergamonti et al mentioning Elder, 1984, Horie, 2013).

In Fig.1 of Bergamonti and coworkers we can find the FTIR transmission spectrum. The researchers tell that "Beeswax, lanolin, carnauba wax and candelilla wax (Figure 1a) show barely visible bands due to the OH stretching vibrations of alcohols, hydroxyl-esters and free fatty acids (marked by asterisks), absent in spermaceti wax. In addition, in beeswax and carnauba wax, the ν(C=O) vibrational bands at 1708 and 1693 cm^{-1} associated with free fatty acids are also observed. … Medium-weak bands, only detectable in the FTIR spectrum of carnauba wax at 1634, 1607, 1515 and 834 cm^{-1}, are attributed to the skeletal ring breathing modes of aromatic groups. … The formulated candelilla, which is a mixture of glyceryl stearate and lesser amounts of natural waxes, also exhibits the strong and wide bands associated with the OH stretching vibrations at 3296 and 3233 cm^{-1} and the band due to the C-O stretching at 1046 cm^{-1} belonging to glyceryl stearate" (Bergamonti et al., see please references therein). Bergamonti and coworkers continue with the Raman spectra of all waxes they consider and provide spectra in their Figure 2a,b. The spectra are "dominated by the strong bands related to the CH_x stretching vibrations: the bands at 2879 cm^{-1} and 2846 cm^{-1} are attributed to the symmetric stretching vibrations of methyl and methylene groups, respectively, and the weak bands at 2957 and 2929 cm^{-1} are assigned to the corresponding antisymmetric modes. The medium-weak peak at 2720 cm^{-1} is due to a combination of the stretching vibrational modes of methyl groups associated with CH_2" (see please the further discussion of the Raman spectra in Bergamonti et al, and the references therein).
"Carnauba wax is a complex mixture of the esters of fatty acids with linear long-chain alcohols and unsaturated hydrocarbons. In the region of CH_x stretching vibrations, we notice the vinyl vibrations at 3068 cm^{-1}. The C=C stretching mode occurs at 1631 cm^{-1} (in cis configuration) and 1610 cm^{-1} (isolated). The presence of the free fatty acid is confirmed by the ν (C=O) band at 1714 cm^{-1}" (Bergamonti et al., mentioning Regert et al., 2001).
After further investigations, the researchers tell that "Carnauba contains saturated fatty acids with even chain length ranging from 16 to 28 carbon atoms, among which behenic acid (C22) and lignoceric acid (C24) were the main components, and long-chain alcohols (C22–C30), triacontanol being the most abundant, in agreement with the results of other authors" (see please the references given by Bergamonti et al., 2022).

From a Database of ATR spectra

In the Database of ATR-FT-IR spectra of various materials, Institute of Chemistry University of Tartu, Estonia, we can find a collection of over 150 spectra of materials related to cultural heritage and conservation science (Vahur et al., 2016). The link https://spectra.chem.ut.ee/paint/binders/ allows us to examine the spectra of the 'binders'. We can find oils, proteins, carbohydrates and waxes (Beeswax, Candelilla wax, bleached Carnauba wax, Polyethylene wax and Shellac Wax). Carnauba Wax spectrum is at https://spectra.chem.ut.ee/paint/binders/carnauba-wax-bleached/ .
Peaks are given at (cm^{-1}):
518, 581, 719, 730, 831, 891, 921, 956, 983, 1037, 1114, 1168, 1201, 1263, 1309, 1377, 1414, 1463, 1472, 1515, 1589, 1606, 1634, 1717, 1735, 2847, 2914, and 2953.
Let us remember that the ATR-IR spectroscopic technique uses infrared light to analyze the chemical structure of a sample. 'ATR' means 'Attenuated Total Reflection'. Therefore, in this spectroscopic technique, the light undergoes multiple internal reflections within a crystal, creating an evanescent wave that penetrates the sample surface, providing valuable molecular information. The evanescent wave interacts with the sample, and the reflected light is then analyzed by the FTIR spectrometer (see the discussion in Sparavigna, 2024, DOI https://dx.doi.org/10.2139/ssrn.4993668).

From the Database by Michael Toffolo

Here we propose the ATR-IR 'fingerprint' of Carnauba Wax, according to data from the "FTIR spectral library of the major components of archaeological sediments", by Michael Toffolo (Project leader), released under Creative Commons Attribution 4.0 International, available https://zenodo.org/records/14170891. The Zenodo page tells us that "Spectra were collected using a Thermo Scientific Nicolet iS5 spectrometer equipped with an iD1 transmission compartment in the 4000-400 cm^{-1} range at 4 cm^{-1} resolution, and in 32 scans. Spectra were collected with the same instrument and settings in ATR mode using an iD7 ATR diamond crystal compartment. Spectra are available in .spa and .csv formats" (Toffolo, 2024).

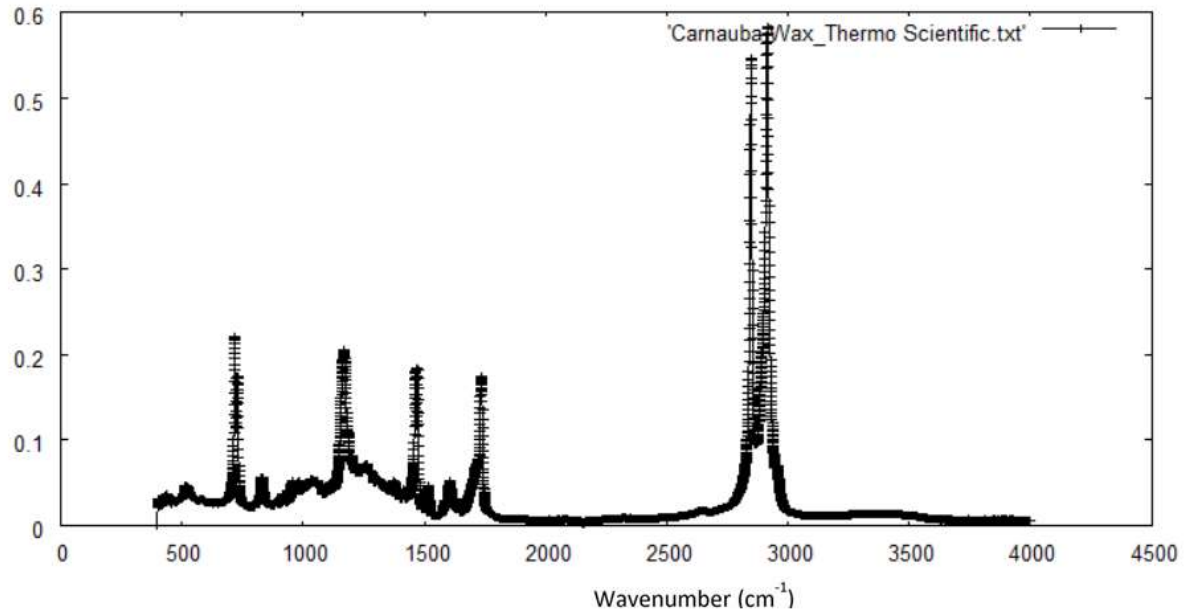

Fig.1 – Carnauba Wax ATR spectrum, courtesy Michael Toffolo (Project leader), released under Creative Commons Attribution 4.0 International, https://zenodo.org/records/14170891

Here we use the term "fingerprint" as it was proposed in relation to the Raman spectroscopy. It seems that this term first appeared in an article published in 1947 about the Raman spectra of hydrocarbons by Fenske and coworkers. Fenske et al., 1947, wrote that the "Raman lines, are characteristic of the substance illuminated and are therefore a "fingerprint" of that substance". From that time on, the points of identification, such as positions of peaks, shoulders and valleys create the characteristic spectral pattern which is known as the "Raman fingerprint" of a given material. Of course, if we have the recorded data, we can decompose the spectrum in components, that is, we can perform a 'deconvolution'. Then, the fingerprint can be characterized not only by the positions of the peaks and shoulders, but also by the parameters related to the functions occurring in the deconvolution. In fact, we can have an "extended fingerprint" of the material. For paraffin ATR-IR we propose an extended fingerprint, as we did before, for augelite and albite minerals. The deconvolution of the spectrum is proposed determined by means of asymmetric q-Gaussian functions, that is the q-BWF functions. These functions (q-Breit-Wigner-Fano functions)

have been proposed by Sparavigna in 2023 and represent the generalization in the framework of Tsallis statistics of the Breit-Wigner-Fano functions. Deconvolutions are obtained using Fityk software (Wojdyr, 2010).

q-Gaussian function and its asymmetric q-BWF form

The fitting of Raman spectra with q-Gaussian line shapes has been proposed for the first time https://www.ijsciences.com/pub/article/2671 by A. C. Sparavigna. The q-Gaussian line shape is a function based on the Tsallis q-form of the exponential function (Tsallis, 1988). This exponential form is characterized by a q-parameter. When q is equal to 2, we have the Lorentzian function. If q is close to 1, we have a Gaussian function. For values of q between 1 and 2, we have a bell-shaped symmetric function with power-law wings ranging from Gaussian to Lorentzian tails.

The q-Gaussian is given as $f(x) = Ce_q(-\gamma x^2)$, where $e_q(.)$ is the q-exponential function and C a scale constant (Hanel et al., 2009). The q-exponential has expression: $e_q(u) = [1 + (1-q)u]^{1/(1-q)}$. For spectroscopy, we write the q-Gaussian function with the center of the band at x_o:

$$q\text{-}Gaussian = Cexp_q(-\gamma(x-x_o)^2) = C\,[1 + (q-1)\gamma(x-x_o)^2]^{1/(1-q)}.$$

We can apply q-Gaussian functions by means of Fityk software. In Fityk, a q-Gaussian function can be defined in the following manner:

```
define Qgau(height, center, hwhm, q=1.5) = height*(1+(q-1)*((x-center)/hwhm)^2)^(1/(1-q))
```

where q=1.5 is the initial guessed value of the q-parameter. Parameter hwhm is the half width at half maximum of the line, in the case of a Lorentzian function. In fact, when q=2, the q-Gaussian turns into a Lorentzian function, that we can find defined in Fityk as:

```
Lorentzian(height, center, hwhm) = height/(1+((x-center)/hwhm)^2)
```

When q is close to 1, the q-Gaussian becomes a Gaussian function.

In Fityk, to define a function, use please Session > New Script > Blank Fityk Script

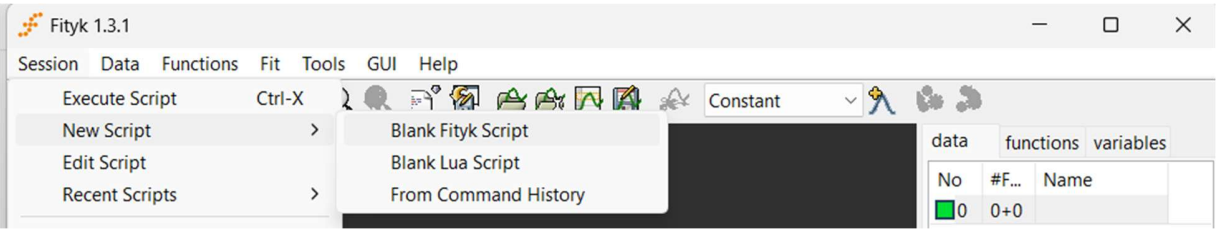

In the Blank Fityk Script paste the “define” of the function, for instance the Qgau given above.

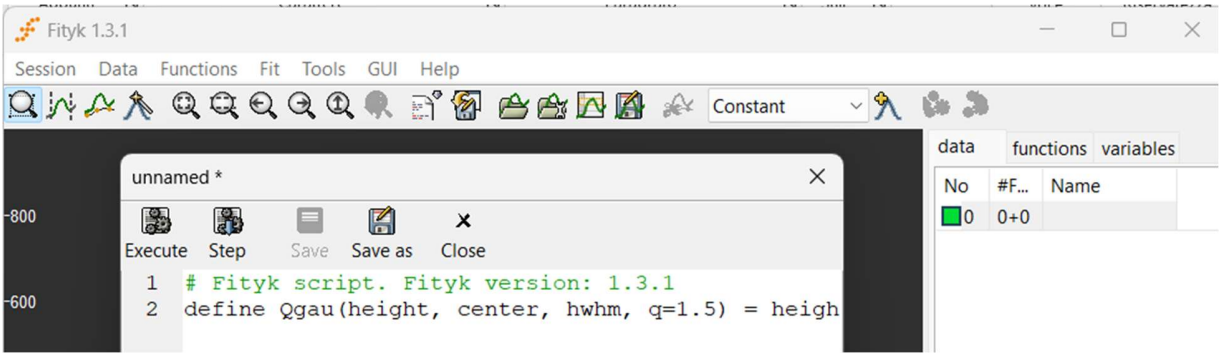

Then, save the Script, and execute it. Using Functions > Definition Manager, in the list of the functions, it will be the q-Gaussian function too.

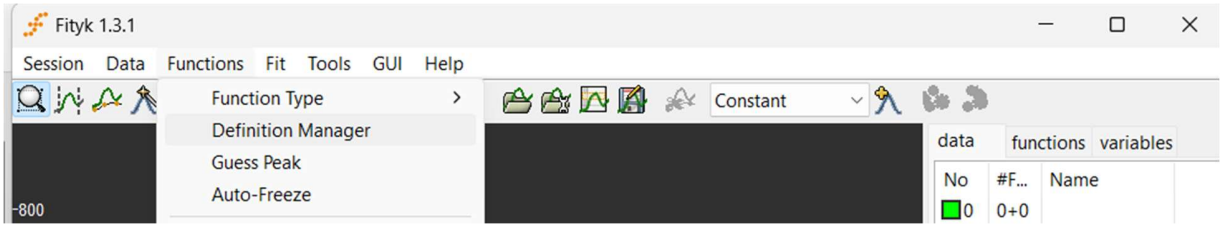

As shown on many occasions, the q-Gaussians are suitable for fitting Raman spectra (by examples proposed in SSRN https://papers.ssrn.com/sol3/papers.cfm?abstract_id=4445044 to the SERS cases, https://chemrxiv.org/engage/chemrxiv/article-details/65092658b6ab98a41cb436e4, for instance). For applying the q-Gaussian functions to the asymmetric bands , https://zenodo.org/records/14220559 , we can define also an asymmetric function, turning the Breit-Wigner-Fano (BWF) function into a q-BWF function (Sparavigna, 2023). Let us write the BWF as follows:

$$\mathrm{BWF}(x) = C\frac{\left[1-\xi\gamma^{1/2}(x-x_o)\right]^2}{\left[1+\gamma(x-x_o)^2\right]}$$

When asymmetry parameter ξ is zero, BWF becomes a symmetric Lorentzian function. Note that the center of the line does not correspond to the position of the peak of the function. As in Sparavigna, 2023, https://zenodo.org/records/8356165 , we can define the q-BWF function in the following manner:

$$\text{q-BWF} = C\left[1-\xi\gamma^{1/2}(q-1)^{1/2}(x-x_o)\right]^2\left[1+(q-1)\gamma(x-x_o)^2\right]^{1/(1-q)}$$

In fact, the Lorentzian function is substituted by a q-Gaussian function.
In Fityk, the q-Breit-Wigner-Fano (q-BWF)
https://iris.polito.it/retrieve/e7985054-588f-4116-843f-f9d2b5296533/asymm-q.pdf
can be defined as:

Qbreit(height, center, hwhm, q=1.5, xi=0.1) = (1-xi*(q-1)*(x-center)/hwhm)^2 * height*(1+(q-1)^0.5 *((x-center)/hwhm)^2)^(1/(1-q))

And the BWF can be defined as:

Breit(height, center, hwhm, xi=0.1) = (1-xi*(x-center)/hwhm)^2 * height/(1+((x-center)/hwhm)^2)

Using +xi instead of −xi does not change the fitting results in Fityk.

Spectral deconvolution

In the following part of our work, we provide ATR-IR spectral deconvolutions for Carnauba Wax in the form of screenshots of Fityk software, where the green dots are data, red curves are the q-BWF components (large components) and Gaussian functions (small components), yellow curve the sum of components. In the lower part of the screenshot, the misfit is given (difference between data and yellow curve). We decided to use the Gaussian functions for small components in order to have a faster deconvolution.

Data are from the "FTIR spectral library of the major components of archaeological sediments", by Michael Toffolo (Project leader), released under Creative Commons Attribution 4.0 International, available https://zenodo.org/records/14170891 .

Supplementary material is providing the Fityk file. At DOI: 10.5281/zenodo.15183001

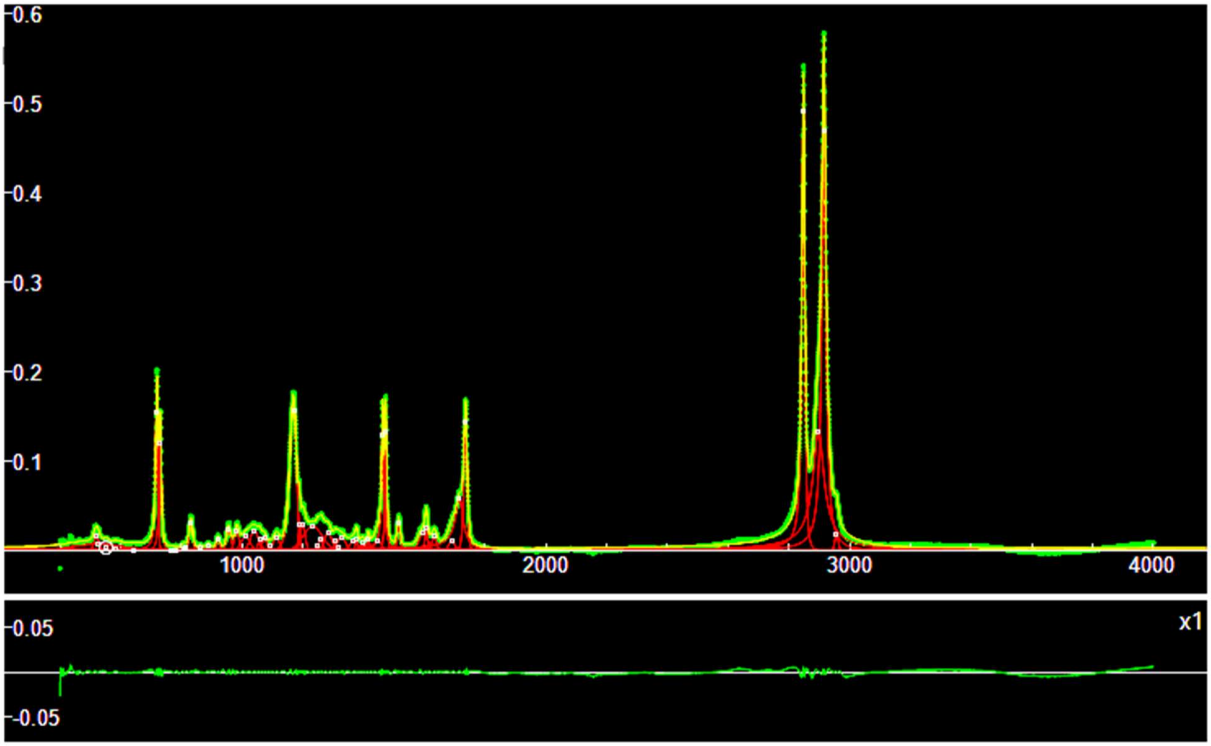

Fig.1: The complete spectrum

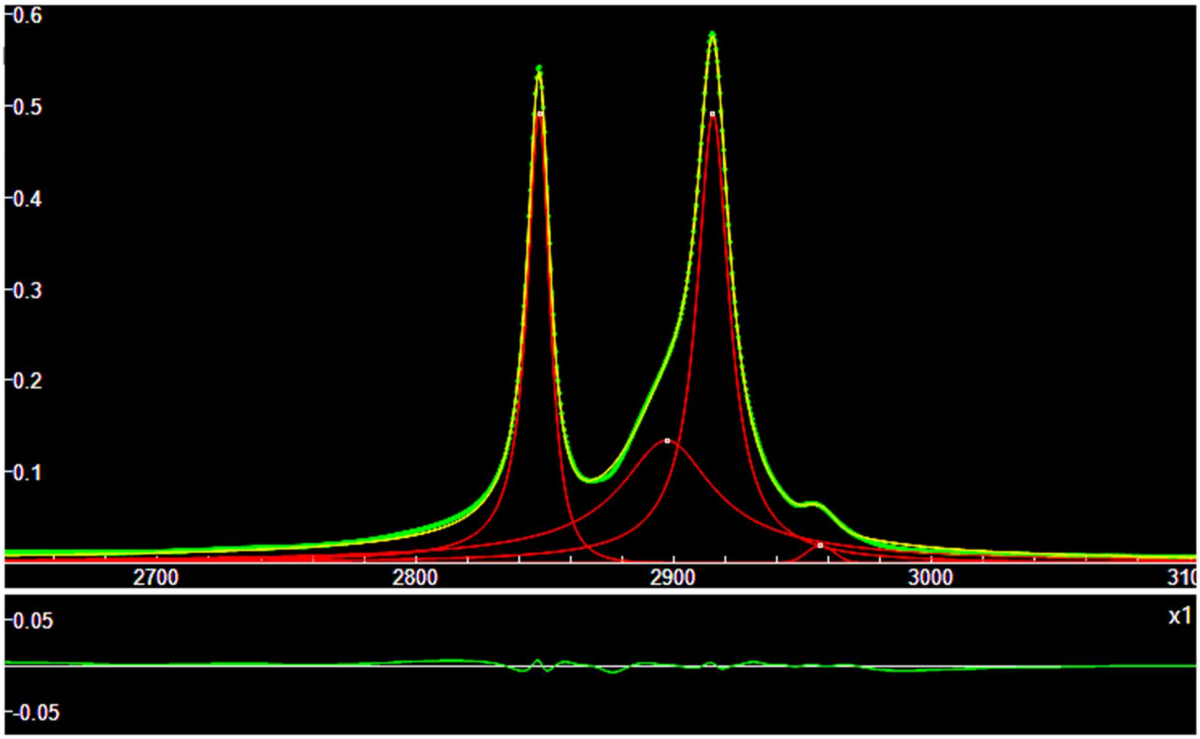

Fig.2: Detail of the deconvolution. Three q-BWF functions are shown.

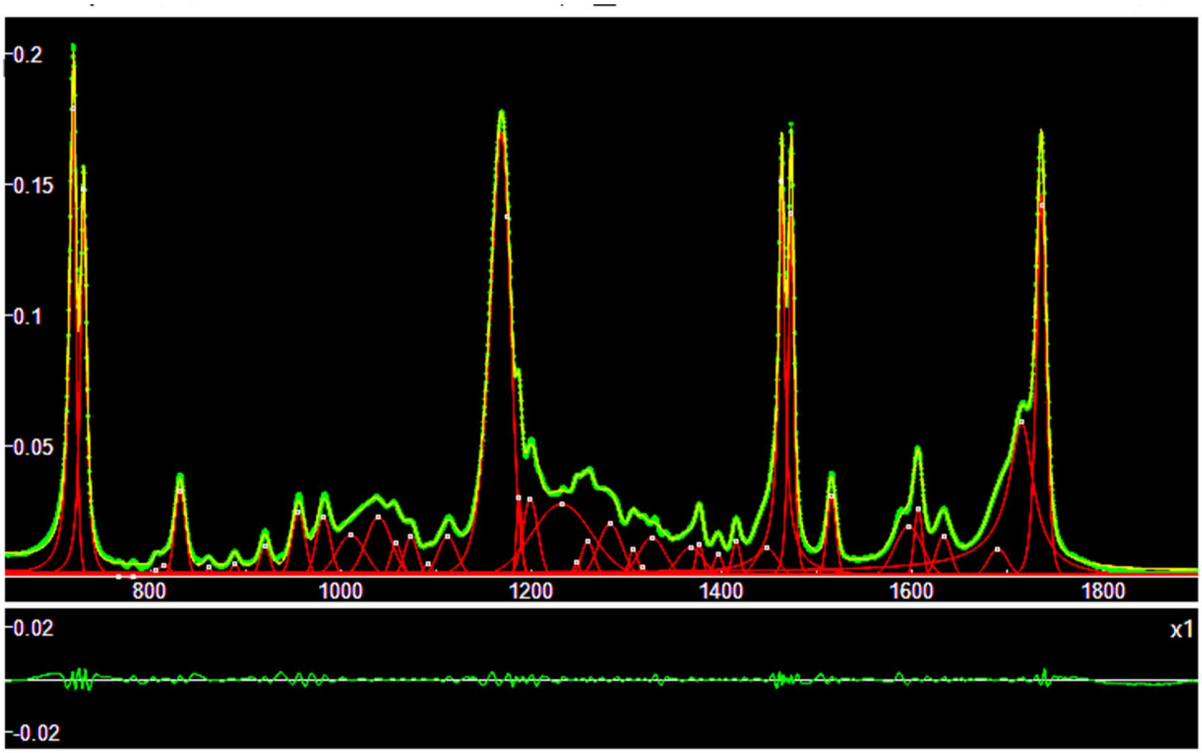

Fig.3: Another part of the spectrum. The larger components are q-BWF functions, the smaller one are Gaussians.

From the figures given above, we can see that the q-BWF functions are asymmetric and then with centers that do not coincide with the peak of the function.
Let us consider the positions of the peaks. The peaks of the q-BWF function are in bold numbers. They are (in cm^{-1}):

520, 552, **719**, **730**, 831, 888, 920, 955, 981, 1039, 1057, 1073, 1112, **1168**, 1187, 1199, 1232, 1259, 1282, 1307, 1326, 1376, 1396, 1415, 1447, **1463**, **1473**, 1515, 1591, 1606, 1632, 1689, **1715**, **1736**, **2848**, **2897**, **2915**, 2957

Let us compare these peaks with those given by Vahur et al., 2016). Peaks are given at (cm^{-1}):
518, 581, 719, 730, 831, 891, 921, 956, 983, 1037, 1114, 1168, 1201, 1263, 1309, 1377, 1414, 1463, 1472, 1515, 1589, 1606, 1634, 1717, 1735, 2847, 2914, 2953.

In https://zenodo.org/records/15167750 we have proposed the q-BWF functions deconvolution of ATR-IR paraffin spectrum. The data given there are useful for comparison, besides the following references: Brown et al., 1954, Chatzipanagis et al., 2024, Edwards and Falk, 1997, Jamwal et al., 2020, Jiménez et al., 2006, Khanifah et al., 2018, MacPhail et al. 1984, and Zheng and Du, 2006.

References

1. Bergamonti, L., Cirlini, M., Graiff, C., Lottici, P. P., Palla, G., & Casoli, A. (2022). Characterization of waxes in the Roman wall paintings of the Herculaneum Site (Italy). Applied Sciences, 12(21), 11264.
2. Brown, J. K., Sheppard, N., & Simpson, D. M. (1954). The interpretation of the infra-red and Raman spectra of the n-paraffins. Philosophical Transactions of the Royal Society of London. Series A, Mathematical and Physical Sciences, 247(922), 35-58.
3. Calovi, M., & Rossi, S. (2023). Synergistic contribution of bio-based additives in wood paint: The combined effect of pigment deriving from spirulina and multifunctional filler based on carnauba wax. Progress in Organic Coatings, 182, 107713.
4. Chatzipanagis, K., Omar, J., & Sanfeliu, A. B. (2024). Assessment of Beeswax Adulteration by Paraffin and Stearic Acid Using ATR-IR Spectroscopy and Multivariate Statistics—An Analytical Method to Detect Fraud. Foods, 13(2), 245.
5. Da Costa, A. A., Marques, M. P. M., & De Carvalho, L. B. (2004). Intra-versus interchain interactions in α, ω-polyamines: a Raman spectroscopy study. Vibrational spectroscopy, 35(1-2), 165-171.
6. de Freitas, C. A. S., de Sousa, P. H. M., Soares, D. J., da Silva, J. Y. G., Benjamin, S. R., & Guedes, M. I. F. (2019). Carnauba wax uses in food–A review. Food chemistry, 291, 38-48.
7. Devi, L. S., Kalita, S., Mukherjee, A., & Kumar, S. (2022). Carnauba wax-based composite films and coatings: Recent advancement in prolonging postharvest shelf-life of fruits and vegetables. Trends in Food Science & Technology, 129, 296-305.
8. dos Santos, A.D.A., Matos, L.C., Mendonça, M.C., do Lago, R.C., dos Santos Muguet, M.C., Damásio, R.A.P., Ponzecchi, A., Soares, J.R., Sanadi, A.R., & Tonoli, G.H.D.

(2023). Evaluation of paper coated with cationic starch and carnauba wax mixtures regarding barrier properties. Industrial Crops and Products, 203, p.117177.
9. Elder, R. L. (1984). Final report on the safety assessment of candelilla wax, carnauba wax, japan wax, and beeswax. Int J Toxicol, 3(3), 1-41.
10. Edwards, H. G. M., & Falk, M. J. P. (1997). Fourier-transform Raman spectroscopic study of unsaturated and saturated waxes. Spectrochimica Acta Part A: Molecular and Biomolecular Spectroscopy, 53(14), 2685-2694.
11. Fenske, M. R., Braun, W. G., Wiegand, R. V., Quiggle, D., McCormick, R., & Rank, D. H. (1947). Raman spectra of hydrocarbons. Analytical Chemistry, 19(10), 700-765.
12. Hanel, R., Thurner, S., & Tsallis, C. (2009). Limit distributions of scale-invariant probabilistic models of correlated random variables with the q-Gaussian as an explicit example. The European Physical Journal B, 72(2), 263.
13. Horie, C. V. (2013). Materials for conservation. Routledge.
14. Jamwal, R., Kumari, S., Dhaulaniya, A. S., Balan, B., & Singh, D. K. (2020). Application of ATR-FTIR spectroscopy along with regression modelling for the detection of adulteration of virgin coconut oil with paraffin oil. LWT, 118, 108754.
15. Jiménez, J. J., Bernal, J. L., del Nozal, M. J., Martín, M. T., & Bernal, J. (2006). Sample preparation methods for beeswax characterization by gas chromatography with flame ionization detection. Journal of Chromatography A, 1129(2), 262-272.
16. Kalyanasundaram, K., & Thomas, J. K. (1976). The conformational state of surfactants in the solid state and in micellar form. A laser-excited Raman scattering study. The Journal of Physical Chemistry, 80(13), 1462-1473.
17. Khanifah, L., Widodo, S., Widarto, W., Putra, N. M. D., & Satrio, A. (2018). Characteristics of paraffin shielding of kartini reactor, Yogyakarta. AJSTD 35, 195–198. doi: 10.29037/ajstd.526
18. MacPhail, R. A., Strauss, H. L., Snyder, R. G., & Elliger, C. A. (1984). Carbon-hydrogen stretching modes and the structure of n-alkyl chains. 2. Long, all-trans chains. The journal of physical chemistry, 88(3), 334-341.
19. Meier, R. J. (2002). Studying the length of trans conformational sequences in polyethylene using Raman spectroscopy: a computational study. Polymer, 43(2), 517-522.
20. Mendonça, M.C., Durães, A.F.S., dos Santos, A.D.A., Matos, L.C., Mascarenhas, A.R.P., Scatolino, M.V., Martins, C.C.N., Damásio, R.A.P., Muguet, M.C.S., & Tonoli, G.H.D. (2024). Natural rubber, cellulose micro/nanofibrils and carnauba wax: renewable and low-cost coatings improving the barrier properties in papers. Cellulose, 31(15), pp.9413-9433.
21. Mills, J., & White, R. (2012). Organic chemistry of museum objects. Routledge.
22. Pashova, S. (2023). Application of plant waxes in edible coatings. Coatings, 13(5), 911.
23. Regert, M., Colinart, S., Degrand, L., & Decavallas, O. (2001). Chemical alteration and use of beeswax through time: accelerated ageing tests and analysis of archaeological samples from various environmental contexts. Archaeometry, 43(4), 549-569.
24. Sparavigna, A. C. (2023). SERS Spectral Bands of L-Cysteine, Cysteamine and Homocysteine Fitted by Tsallis q-Gaussian Functions. International Journal of Sciences, 12(09), 14-24.
25. Sparavigna, A. C. (2023). q-Gaussian Tsallis Line Shapes and Raman Spectral Bands. International Journal of Sciences, 12(03), 27-40.
26. Sparavigna, A. C. (2023). q-Gaussian Tsallis Line Shapes for Raman Spectroscopy (June 7, 2023). SSRN Electronic Journal. DOI: 10.2139/ssrn.4445044

27. Sparavigna A. C. (2023). Tsallis q-Gaussian function as fitting lineshape for Graphite Raman bands. ChemRxiv. Cambridge: Cambridge Open Engage; 2023.
28. Sparavigna, A. C. (2023). Asymmetric q-Gaussian functions generalizing the Breit-Wigner-Fano functions. Zenodo. https://doi.org/10.5281/zenodo.8356165
29. Sparavigna, A. C. (2024). Raman and Attenuated Total Reflectance Infrared RRUFF Spectra: some cases of deconvolution with q-Gaussians and q-BWF functions. SSRN Electronic Journal, DOI: 10.2139/ssrn.4993668
30. Sparavigna, A. C. (2024). Atlas of Metabolite SERS Fingerprints obtained by means of q-Gaussian deconvolutions and Fityk Software. ChemRxiv. DOI: 10.26434/chemrxiv-2024-85l19-v2
31. Sparavigna, A. C. (2024). Hydroxyl-Stretching Region in the Raman Broad Scans on Minerals of the Vivianite Group (Vivianite, Baricite, Bobierrite, Annabergite, Erythrite). International Journal of Sciences, 13(08), 23-36.
32. Sparavigna, A. C. (2025). Albite Feldspar Mineral Raman and ATR-IR Fingerprints obtained with q-Gaussian and q-BWF deconvolutions made by means of Fityk Software. Zenodo. https://doi.org/10.5281/zenodo.14743007
33. Sparavigna, A. C. (2025). Augelite Raman and ATR-IR Fingerprints obtained with q-Gaussian and q-BWF deconvolutions made by means of Fityk Software. Zenodo. https://doi.org/10.5281/zenodo.15007192
34. Sparavigna, A. C. (2025). Augelite Raman and ATR-IR spectral deconvolutions in Fityk Software .fit and .peaks files [Data set]. Zenodo. https://doi.org/10.5281/zenodo.15007133
35. Svečnjak, L., Baranović, G., Vinceković, M., Prđun, S., Bubalo, D., & Tlak Gajger, I. (2015). An approach for routine analytical detection of beeswax adulteration using FTIR-ATR spectroscopy. Journal of Apicultural Science, 59(2), 37–49. doi:10.1515/JAS-2015-0018
36. Tinto, W. F., Elufioye, T. O., & Roach, J. (2017). Chapter 22. Waxes, Editor (s): Simone Badal, Rupika Delgoda, Pharmacognosy. Academic Press, Pages 443-455, ISBN 9780128021040, https://doi.org/10.1016/B978-0-12-802104-0.00022-6
37. Toffolo, M. (2024). FTIR spectral library of the major components of archaeological sediments [Data set]. Zenodo. https://doi.org/10.5281/zenodo.14170891
38. Tsallis, C. (1988). Possible generalization of Boltzmann-Gibbs statistics. Journal of statistical physics, 52, 479-487.
39. Tulloch, A. P. (1980). Beeswax—composition and analysis. Bee world, 61(2), 47-62.
40. Vahur, S., Teearu, A., Peets, P., Joosu, L., & Leito, I. (2016). ATR-FT-IR spectral collection of conservation materials in the extended region of 4000-80 cm–1. Analytical and Bioanalytical Chemistry, 408, 3373-3379.
41. Wojdyr, M. (2010). Fityk: a general-purpose peak fitting program. Journal of applied crystallography, 43(5), 1126-1128.
42. Zheng, M., & Du, W. (2006). Phase behavior, conformations, thermodynamic properties, and molecular motion of multicomponent paraffin waxes: A Raman spectroscopy study. Vibrational Spectroscopy, 40(2), 219-224.